Lasers in Manufacturing Conference 2019

Study of laser cold-wire welding of thick aluminum sheets along different gap size and laser-to-wire position

F. Mirakhorli[a*], F. Nadeau[a], G. C.-Guillemette[b], R. Fakir[b]

[a]*National Research Council Canada, Saguenay, Québec, Canada G7H 8C3*
[b]*Bombardier Transport Canada Inc, La Pocatière, Québec, Canada, G0R 1Z0*

Abstract

In recent years, there has been growing interest in joining thick aluminum sheets in various markets such as railcar, shipbuilding and aerospace. Laser cold-wire (LCW) welding was developed in this study to join 5.0 mm thick AA6005-T6 aluminum sheets in butt joint configuration. To investigate the gap bridging ability of LCW technique, a process parameter optimization was performed for three different gaps ranging from (I) 0.25-0.50 mm, (II) 0.50-0.70 mm and (III) 0.70-1.00 mm. The effect of a linear misalignment was also studied by applying a 0.75 mm misalignment (15% of the sheet thickness) during joint preparation. The result of this study showed that the LCW can easily sustain the gap and misalignment tolerances of 0.75 mm. The welded joint integrity with different gaps and misalignments was characterized in terms of the weld bead geometry, defects, macrostructure, hardness and tensile strength.

Keywords: Laser cold-wire welding, gap tolerance, misalignment, thick aluminum sheet.

1. Introduction

Laser welding technology has been developed recently for welding aluminum alloys for lightweight applications due to its interesting characteristics such as high power density, which help to increase the welding speed thus reducing the fusion (FZ) and heat affected zones (HAZ) area, as well as its deep possible penetration. However, the application of autogenous laser welding, especially for thick aluminum sheets, is restricted due to more frequent collapse of keyhole and spatter formation during keyhole laser welding as discussed by Huang et al., 2018. Besides, autogenous laser welding has very low tolerance to seam gap which makes the use of filler wire mandatory for the applications where it is difficult to hold tight part tolerances. To minimise the gap between the sheets in butt joint configuration, strict fit up and clamping

* Corresponding author. Tel.: +1-418-545-5098; fax: +1-418-545-5345.
E-mail address: fatemeh.mirakhorli@cnrc-nrc.gc.ca

system is required which increase the implementation costs of laser welding technology. Very tight tolerance of laser welding in comparison with other conventional fusion welding processes such as gas metal arc welding (GMAW) is a main drawback for certain applications. Several researches have been performed to increase the gap tolerance of joints, in laser-based welding techniques such as hybrid laser-arc welding (HLAW) and laser cold-wire welding as reported by Aalderink et al., 2010, Wang et al., 2013 and 2009. The results of these studies show that HLAW welding technique can increase gap-bridging ability of 2.0 mm thick aluminum alloy up to 1.0 mm and reduce the weld surface imperfections such as undercuts or underfills. Aalderink et al., 2010 research study on gap bridging of laser based processes showed that the gap tolerance of laser cold-wire process increased significantly compared to autogenous laser welding and can increase up to 1.1 mm gap bridging in 2.1 mm thick aluminum sheets. Although several studies have been performed on parameters optimisation of LCW techniques and its influence on gap bridging in relatively thin aluminum sheets (up to 2 mm), no or very few research studies have been performed on the effect of LCW welding process on gap bridging of thick aluminum sheets and on microstructure and mechanical properties of welded joints. Single-pass laser cold-wire welding of thick section AA6061-T6 aluminum sheets has been studied by these authors previously in terms of process parameter optimisation and the effect of laser beam mode on mechanical properties by Mirakhorli et al., 2018. However, there is still a lack of understanding on maximum gap tolerance of LCW for welding thick aluminum alloys in laser keyhole mode and the effect of gap tolerance on post-weld mechanical properties. To our knowledge, no research has been published in this area. In this study, the gap and misalignment tolerances of LCW welding technique on 5.0 mm thick aluminum sheets were investigated in butt joint configuration, using single pass welding. The welding process parameters were developed for three different gap ranges of small (up to 0.5 mm), (II) medium (up to 0.7 mm) and (III) large (up to 1.0 mm,). The main challenge during process setup is the precise alignment of the filler wire relative to the laser beam which is discussed further using a high speed camera. The optimum parameters have been found for each gap ranges and their effect on microstructure and mechanical properties has been investigated. Also, a linear misalignment up to 0.75 mm (15% of the sheet thickness, chosen based on ISO 13919-2 quality level C as the acceptable limit) has been applied to study the tolerance of LCW welding process to misalignment. For this study, medium size gap has been chosen and the effect of misalignment has been studied on process stability, weld bead geometry and mechanical properties.

2. Experimental procedure

Laser welding was performed using a pulsed TRUMPF TRUDISK 10 kW solid-state disk laser with a wavelength of 1030 nm. Laser beam was scanned using Primes FocusMonitor instrument. The defocus distance of 4 mm inside the specimen was used for all the experiments. The laser beam diameter at different focal positions as well as laser beam intensity distribution at -4 mm defocus surface are presented in figure 1 (a) and (b) respectively. The beam had a nominal focal spot diameter of 0.87 mm. The approximate beam diameter at -4 defocus distance was 1.07 mm with a Gaussian intensity distribution shown in figure 1(b). The laser head was inclined 5° from the vertical plane perpendicular to the welding direction to protect the optic system against back reflection during laser welding. The filler wire was added using a Miller XR wire feeder system in leading configuration as illustrated in figure 2.

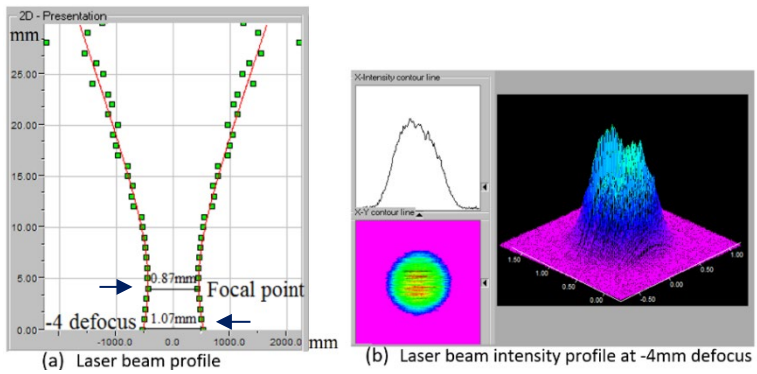

Fig. 1. (a) Laser beam profile at different focal distance and (b) laser beam intensity distribution

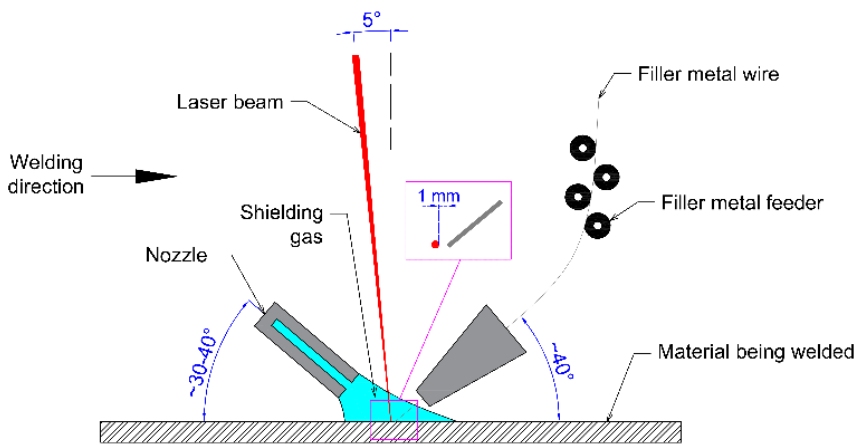

Fig. 2. Schematic diagram of the experimental set-up.

The angle between the filler wire axis and the workpiece surface parallel to the welding direction was ~40° and high purity argon was used as a shielding gas during welding process fed by the nozzle at a flow rate of 23.6 l/min. The shielding gas nozzle was positioned at ~30-40° from the workpiece surface. The laser beam was positioned in the middle of the gap and the filler wire was positioned outside laser beam, 1.0 mm away from laser beam as shown in figure 1. The base material (BM) used in this study was AA6005A-T6 wrought aluminum sheets with dimension of 300 mm (length) × 100 mm (width) × 5 mm (thick). The filler wire used for welding was ER5356, 1.6 mm in diameter. The nominal chemical compositions of AA6005A-T6 and ER5356 filler wire are shown in Table 1. The BM sheets were ground and cleaned with acetone before welding, then fixed within a clamping device in butt joint configuration with three different range of root opening (gap sizes); small gap (0.25-0.5 mm), medium gap (0.5-0.7 mm) and large gap (0.7-1.0 mm).

Table 1. Nominal chemical composition of BM (BS EN 573-3 2009) and filler wire (AWS: A5.10)

Alloy	Mg (wt. %)	Mn (wt. %)	Si (wt. %)	Fe (wt. %)	Zn (wt. %)	Cr (wt. %)	Al (wt. %)
AA6005A	0.40-0.70	0.0- 0.5	0.5-0.9	0.0-.35	0.0-0.2	0.0-0.3	Bal.
ER5356	4.5-5.5	0.05-0.2	0.25	0.4	0.1	0.1	Bal.

To monitor the LCW process in real time, a Phantom high-speed camera using a frame rate of 10000 images per second was used in combination with a 1kW pulse laser source as an illumination source.

An X-ray analysis was made using a YXLON Y.Multiplex 5500M radiographic system to inspect the welded samples to detect porosity through the entire weld length, excluding the start and stop regions. Metallographic specimens were extracted from the middle of each weld and the transverse section of each specimens were grinded using SiC papers up to 1200 grit, polished using 3 and 1 µm diamond suspensions, then etched in Barker's electrolytic etch (5%HBF4 solution) at 30 V for 2 minutes to reveal the grain structure. The microstructure of the welds was examined using an optical microscope (OM) (Olympus BX51M) and a Hitachi SU-70 field emission gun scanning electron microscopy (FEG-SEM). Microhardness profiles across the weld center were measured using a Clemex CMT Vickers micro-indentation machine. Tensile tests were conducted according to the ASTM B557 standard.

2.1. Welding parameters

Process parameter optimization was performed for each three different range of root opening and the main process parameters are presented in table 2. The maximum laser power of 10 kW was used for all the trials and the laser average power was adjust to achieve the required energy to achieve a full penetration. To bridge a larger gap size, it requires a larger volume of material or filler metal consumption which can be achieved by increasing the wire feed speed and it also needs more laser energy to melt the filler wire. Besides, with increasing the gap size, there is greater risk that a part of the laser energy is lost by passing through the gap particularly at larger gaps which is as large as the laser beam diameter. To compensate the loss of energy through the gap, the laser travel speed was reduced ~ 10% from 3.00 m/min to 2.75 m/min and the pulse shape was modified to reach an increase of 17% in pulse energy. The filler metal consumption was calculated as described by Mirakhorli et al., 2017.

Table 2. Laser cold-wire parameters for different gap tolerance

Gap range mm	Peak power (kW)	Travel speed (m/min)	Average power (kW)	Pulse duration (ms)	Pulse energy (J)	Wire feed Speed (m/min)	filler metal consumption (g/m)
Small gap 0.3-0.5 mm	10	3.0	6.5	20	134	3.0	5.4
Medium gap 0.5-0.7 mm	10	3.0	6.5	20	134	5.0	9.1
Large gap 0.7-1 mm	10	2.7	7.7	20	161	6.5	13.1

3. Results and Discussion

3.1 Effect of laser -to -wire position on weld bead geometry

The interaction between the laser beam and the filler wire during LCW welding process was monitored using a high speed camera during this study and the results show that the precise alignment between the two is very critical during this process. Even small deviations of the filler wire from the gap center or from the laser beam can lead to unacceptable weld seams. Figure 3 shows the main critical alignment parameters during LCW set up and the possible defects related to each condition listed in table 3. The optimum position of the filler wire relative to the laser beam is demonstrated in figure 3(a). The centre of the laser beam should be positioned in the middle of the gap and the wire tip should be at a distance of 1.0 mm from the edge of the laser beam while touching the sheet surface. The keyhole diameter size can reach approximately 1.0-1.2 mm, measured with high speed camera images as shown in figure 3(a), which exceeds up to 10% the actual laser beam size (1.07 mm). The formation of the keyhole during the laser welding process leads to a local surface depression around it. This depression is due to a recoil pressure formation during welding as discussed by Fotovvati et al., 2018 and Semak et al., 1995. This depression around the keyhole during laser welding permits the filler wire to reach a position adjacent to the keyhole front side to melt by laser radiation before moving into the keyhole. If the filler position during the setup is very close to the laser spot or reaches into the laser spot center, as shown in figure 3(b), the filler will interrupt the keyhole stability by closing it or reflecting a noticeable part of laser energy. These would lead to lack of fusion and porosity formation in the weld. If the distance between the wire tip and the laser beam is large, the laser beam will pass through the gap, in the larger gap tolerance, without completely melting the wire and leads to formation of large blowholes as displayed in figure 3(c). This phenomena shows that during LCW welding of thick sheets, the filler metal helps to absorb and transfer the laser energy to the edges of the joint and avoids losing the laser energy through the air gap. Based on this observation, the filler wire with a diameter close to or slightly larger than the air gap is recommended for this configuration. In the smaller gap tolerance, the large distance between the filler wire and the laser beam leads to a lack of filler metal mixture within the molten pool as shown in figure 3(d), since the laser beam is quite bigger than the air gap. The laser energy is absorbed by the base metal but the filler metal cannot reach the laser beam and therefore

cannot melt appropriately which leads to formation of an isolated droplet at the tip of filler wire. This means that at larger filler to laser beam distances, the filler wire cannot reach the laser beam and will be heated just by the laser beam reflection or the melt pool formed in front of the keyhole which is insufficient to melt the filler wire completely and it forms a cold droplet as shown in figure 3(d). This leads to lack of filler metal in the joint and consequently a deep underfill defect.

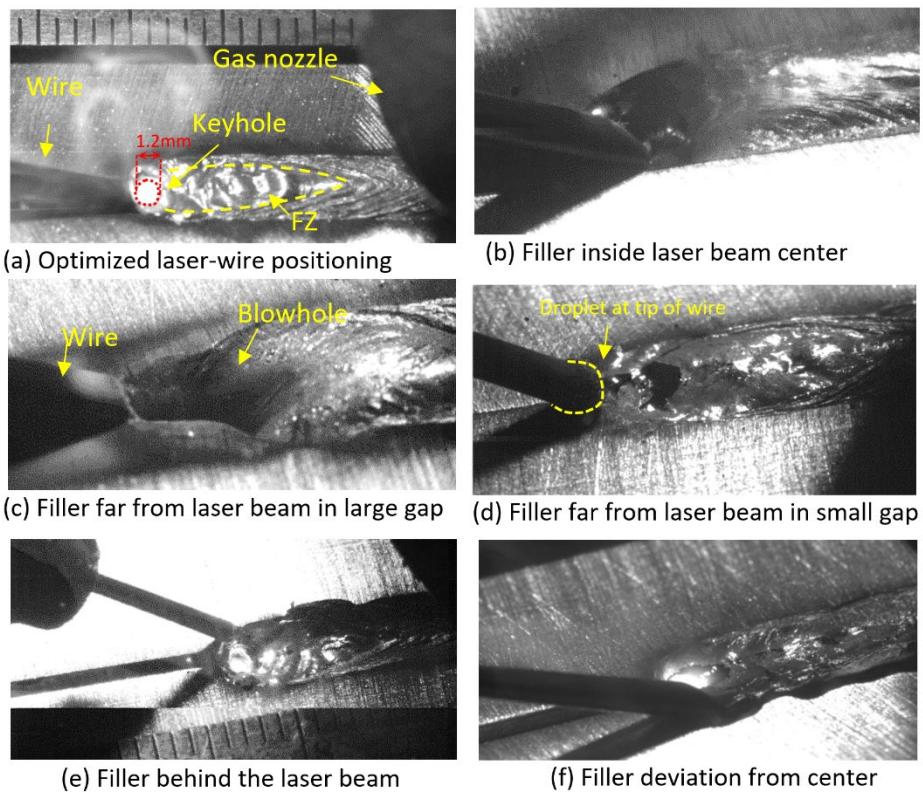

Fig. 3. (a) Relative position between filler metal and laser source for optimized position; (b-f) non-optimized positions

Table 3. Defects related to different laser-to-wire position shown in Fig. 3

Laser-filler position based on Fig.3	Lack of fusion	blowhole	underfill	porosity
a				
b	X			X
c		X	X	
d			X	
e	X			X
f		X	X	

The other possibility is that the wire position is high enough that it crosses over the laser beam and reaches the back side of the fusion zone as displayed in figure 3(e). In this way, the filler metal will block the laser beam and reflects a part of laser energy which would lead to lack of fusion.

The last miss-position between laser and filler metal that was noticed during this study is when the filler metal deviates from the air gap centerline to the left or right of the joint, as shown in figure 3(f). This can happen if the wire is not well positioned at the beginning or during LCW welding or if there are some discontinuities on the sheet edge surfaces that displace the wire from the gap center. This can lead to blowhole formation in large gap or underfill and an overlay defect at a smaller gap since the molten metal does not distribute evenly around molten pool.

3.2 weld geometry and microstructure

Figure 4 shows surface appearances (top and root sides) and X-ray images of welds at different gap tolerances. In all three welding conditions, uniform weld beads with full penetration were achieved. The underfill top surface and undercut at the root surface was less than 0.5 mm (0.05 x thickness of the sheet). The X-ray images show random porosity formation with a fraction of less than 3% over 200 mm weld length and a maximum pore dimension of 1.3 mm, passing the minimum requirement criteria of ISO 13919-2 standard quality class (level B) which is the most stringent level in the mentioned standard. The x-ray images show that less porosity forms at larger gap tolerances compared to the small one.

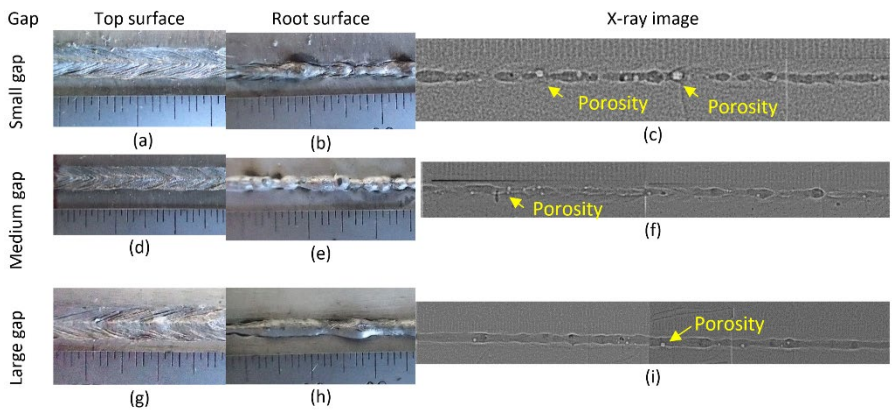

Fig. 4. (a,b,d,e,g,h) Weld beads surface appearances; (c,f,i) corresponding X-ray images

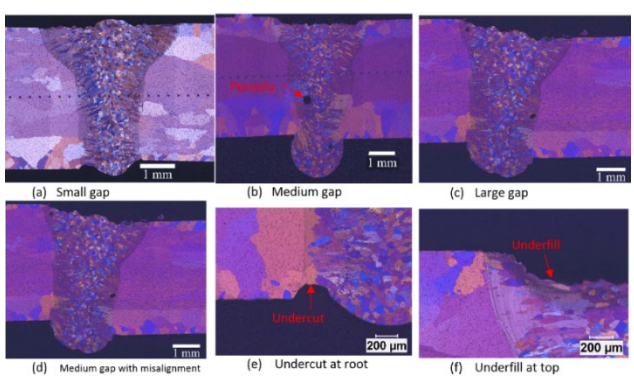

Fig. 5. (a-c) Weld transverse sections for small gap, medium gap, large gap and medium gap with misalignment respectively, (d-f) weld defects

Adding the gap can help porosity escape through it during laser welding. Keyhole collapse is more prone at smaller gap tolerances which captures the vapour inside the molten pool. The weld transverse sections with different gap tolerances as well as misalignment are shown in figure 5. The average width of the weld beads in each air gap tolerances was measured at top, middle and bottom positions. The results show that the weldment with a small gap has the minimum weld width with a value of 2.5 mm which increases with the weld gaps from 2.9 mm to 3.6 mm respectively for medium and large gap sizes. In total, a 19% increase in weld width is observed for the total gap width increase of 56% (from small gap to largest). It is noteworthy that the filler metal consumption was increased just 58% (5.45g/m for small gap to 13.1 g/m for the largest gap as mentioned in table 2) which is compatible with the gap size percentage increase. The microstructures from FZ up to HAZ were very similar at different gap range.

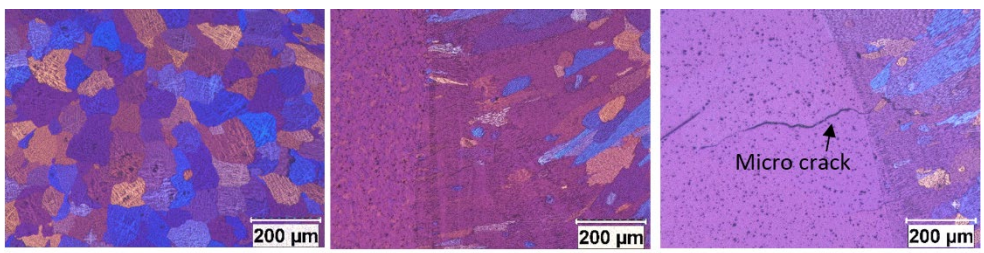

Fig. 6. Weld microstructure in (a) FZ, (b) fusion line, (c) HAZ

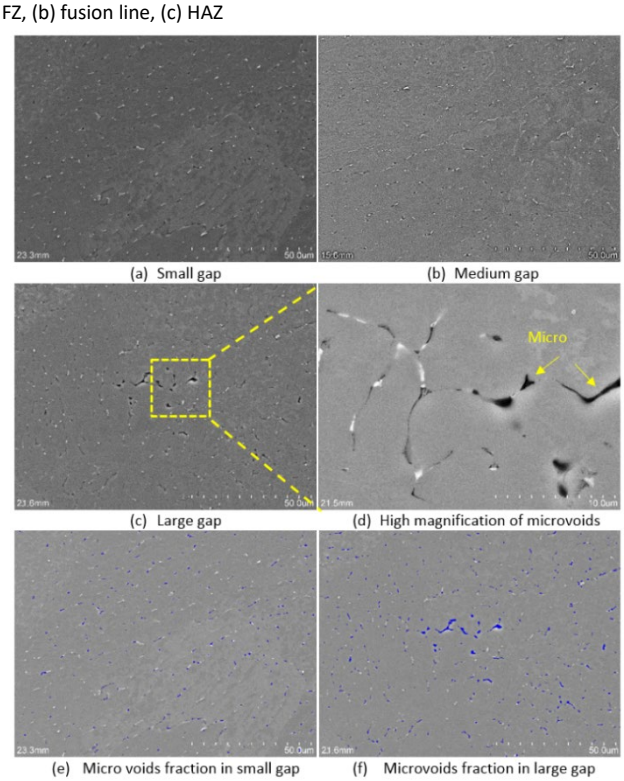

Fig. 7. (a) SEM images in FZ for small gap, (b) medium gap, (c) large gap, (d) microvoids and second particle at high magnification

The FZ exhibited an equiaxed grain structure in the center (figure 6(a)) and a columnar grain structure near fusion line (figure 6(b)). No micro-crack formation was observed within the FZ but some micro-cracks were observed in the HAZ close to fusion line (figure 6(c). These cracks seem to be of the intergranular type which forms in partially melted zone during welding. Böllinghaus, 2018 explained that in Al-Mg-Si aluminum alloy welding, liquid films form between partially melted grains where eutectic constituents with lower melting temperature is found compared to the aluminum matrix. The liquid film will be pulled out by surrounded solidified materials due to thermal strain formed during welding and this leads to liquation cracking in partially melted zone or HAZ. Ivanov et al., 2018, explained in his recent research study on laser welding of Al-Mg-Si alloys that beside the formation of liquid films due to segregation of Mg, Si at grain boundaries, intense plastic straining is responsible for the formation of liquation cracks. Although no micro crack was observed within the FZ, the SEM images at high magnification of 1000X show the formation of microvoids all over the FZ, as shown in figure 7. Similar microvoids were also observed during LCW welding of AA6061-T6 aluminum alloys studied by Mirakhorli et al., 2018.The qualitative measurements show than the fraction of microvoids increased slightly with increasing gap size from 0.3% to 0.7% in small gap to large gap respectively (as shown in figure 7(e) and (f)). These microvoids seems to form at the grain boundary adjacent to eutectic which is enriched in Mg and Si, as observed in higher magnification in figure 7d. These micro voids coalescence and form micro-cracks during mechanical testing that can reduce mechanical properties as reported by Stefanescu et al., 2004.

3.3 Mechanical properties: microhardness and tensile

The hardness profiles across the FZ, HAZs, and BM for welds with different gap tolerances, measured along the mid-thickness of a transverse section, are shown in figures 8(a) through (c). Similar trends were observed for the three gap tolerances. The microhardness reduces in FZ and HAZ compare to BM, with the minimum microhardness found in HAZ II, at 2-4 mm distance from the fusion line

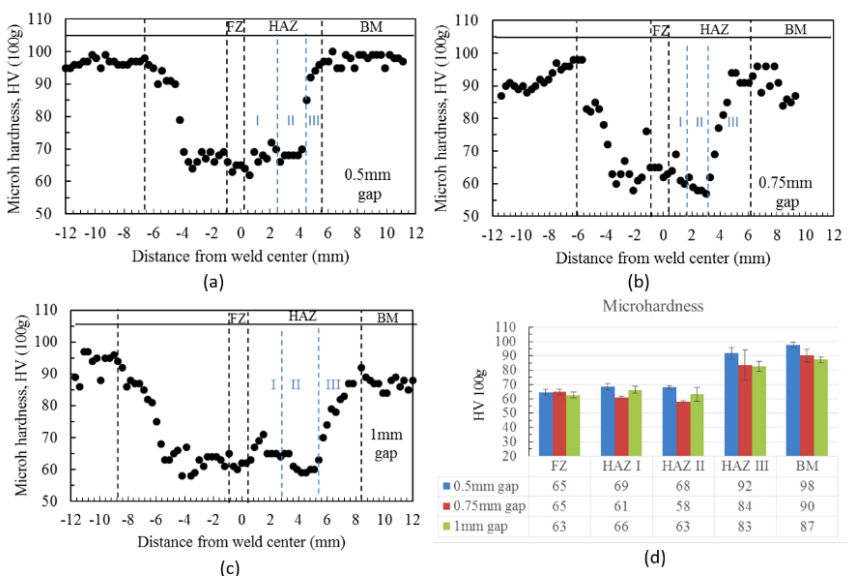

Fig. 8. (a) The hardness profiles for small, (b) medium, (c) large gap tolerances and (d) hardness comparison of different gaps

According to Walter et al., 2014, the maximum reduction in this area can be attributed to over aging during welding thermal cycle. The HAZ I, which is adjacent to 2 mm from the fusion line show microharness of slightly higher than HAZII. This behaviour was also observed during welding of Al-Si-Mg as well as Al-Cu-Li alloys reported by Walter et al., 2014 and Kramer et al., 1992 respectively. According to their research, at this region of HAZ (HAZI), the weld exposes to significant heating, sufficient to put in solution locally and during fast cooling, supersaturated solid solution can occur. The precipitates can form as a result of natural aging which leads to slightly increase the mcirohardness in this zone. The microhardness increases gradually from HAZ II to BM, which is indicated as HAZ III in figure 8, due to the reduction of the peak temperature reached during welding. The fraction of over-aged particles reduces gradually from HAZIII until it reaches to BM which is not affected during welding. In general, a maximum softening of 32% occurred in HAZ II relative to a medium gap size. The average FZ hardness (figure 8(d)) tends to be very similar for all gap tolerances. The variation of the HAZ hardness at different gaps was between 9 to 14% which can be mostly due to variations in the initial BM microhardness which is encountered during the extrusion process. Similar variations in microhardness profiles were detected by Malin, 1995 and Walter, 2014. Transverse tensile properties such as ultimate tensile strength (UTS), yield strength (YS) and percentage of elongation (El. %) were evaluated for different gap tolerances and are listed in figure 9. The average UTS values for all the welds were quite similar (with 5% variation between Min. and Max. values). The average ultimate tensile strength value for all the welds was 187 MPa. The maximum ultimate tensile strength was obtained at a medium gap range with a value of 194 MPa whereas the total gage length elongation at rupture was determined as 4 %. The minimum UTS was obtained at the small gap range with a value of 182 MPa. It is worth mentionning that all the fractures occured at the fusion line and the presence of local softening did not affect the failure location since it did not occur within this area. Geometrical defects such as small underfill at the top surface and undercuts at the root side (shown in figure 5(e) and (f)) have the main influence on failiure occurrence at the fusion line. The tensile strengths for the sample with 0.75 mm misalignment, at medium gap size, was similar to the samples without misaligment (186 MPa). Although the misaligment did not affect the tensile weld properties, it can significantly reduce the fatigue life and fatigue strength of the welds, as explained by Nguyen, 1998 and detailed in the IIW standard.

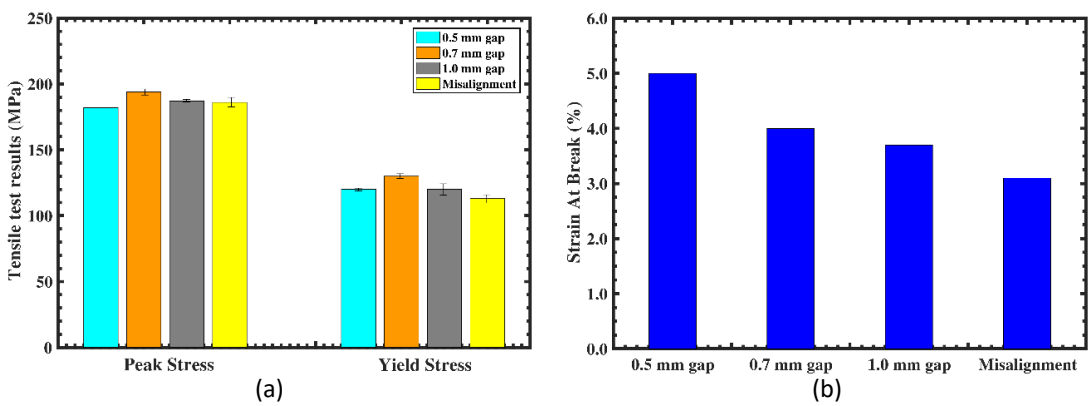

Fig.9. (a) Tensile strengths and (b) strain elongations for different welds gap tolerances and misalignment

Conclusion

Laser cold-wire (LCW) welding process was succesfully used to join 5.0 mm thick AA6005A-T6 alloy in butt joint configuration and the air gap tolerance was enlarged up to 1.0 mm. The main findings were as follows;

1-The relative position between laser and filler metal is a critical parameter to achieve a sound weld during LCW welding. The optimum weld condition was obtained when the laser beam center was in the middle of the gap and when the filler wire tip was 1.0 mm farther from the edge of the laser beam. At shorter laser to filler distances, the laser beam got blocked by the wire and lead to lack of fusion. Blowholes can form at larger gaps, if the laser filler distance is longer than the optimum value.

2- The main imperfections observed in the welds were underfill at the top surface, root undercut, porosity and micro-crack in the HAZ. The porosity level reduced at larger gap size as the air present in the gap helped the porosity to escape during solidification. The micro-cracks formed mainly in the partially melted zone due to the formation of low melting point eutectic constituents. These micro-cracks are promoted by an absence of dilution with the filler metal as well by high local strains occuring at this specific location.

3- The softening in FZ and HAZs occurred after welding with a minimum hardness in the HAZ, at 2-4 mm from the fusion line. This softening was attributed to dissolution of hardening precipitates and overaging upon the welding cycle. The air gap did not show a significant influence on microhardness as well as post-weld tensile strength. The average ultimate tensile and yield strength values for the welds were 187 MPa MPa and 121 MPa respectively. Tensile strength of samples with 0.75 mm misaligment was similar to the situation without misaligment and all the fractures occurred at fusion lines initiating from a geometrical defect, the root undercut.

Acknowledgements

The authors would like to thank Bombardier Transport Canada Inc for their financial support. The technical assistance of M. Larouche (for welding experiments) and H. Grégoire and S. Tu (for metallographic preparation) of National Research Council of Canada, Aluminum Technology Centre (ATC-NRC) is gratefully acknowledged.

References

Huang, L., Hua, X., Wu, D. and Li, F., 2018. Numerical study of keyhole instability and porosity formation mechanism in laser welding of aluminum alloy and steel. Journal of Materials Processing Technology, 252, pp.421-431.

Aalderink, B.J., Pathiraj, B. and Aarts, R.G.K.M., 2010. Seam gap bridging of laser based processes for the welding of aluminum sheets for industrial applications. *The International Journal of Advanced Manufacturing Technology*, *48*(1-4), pp.143-154.

Wang, J.B., Nishimura, H., Katayama, S. and Mizutani, M., 2013. Welding of aluminum alloy by using filler-added laser-arc hybrid welding process. *Welding International*, *27*(2), pp.98-108.

Wang, J.B., Nishimura, H., Fujii, K., Katayama, S. and Mizutani, M., 2009. Study of improvement of gap tolerance in laser MIG arc hybrid welding of aluminum alloy. *Welding International*, *23*(10), pp.723-733.

Mirakhorli, F., Nadeau, F. and Guillemette, G.C., 2018. Single pass laser cold-wire welding of thick section AA6061-T6 aluminum alloy. *Journal of Laser Applications*, *30*(3), p.032421.

DIN, E., 2009. 573-3: Aluminium and aluminium alloys-Chemical composition and form of wrought products-Part 3: Chemical composition and form of products. German version EN, pp.573-3.

ANSI-AWS a5.10. 1999. Specification for Bare Al and Al-alloy welding electrodes and rods

Fotovvati, B., Wayne, S.F., Lewis, G. and Asadi, E., 2018. A review on melt-pool characteristics in laser welding of metals. *Advances in Materials Science and Engineering*, *2018*.

Semak, V.V., West, J.C., Hopkins, J.A., McCay, M.H. and McCay, T.D., 1995, November. Shape and position of keyhole during laser welding. In *International Congress on Applications of Lasers & Electro-Optics* (Vol. 1995, No. 1, pp. 544-552). LIA.

ISO, E., 2003. 13919-2. *Welding–Electron and laser beam welded joints–Guidance on quality levels for imperfections–Part*, *2*.

Böllinghaus, T., Herold, H., Cross, C.E. and Lippold, J.C. eds., 2008. *Hot cracking phenomena in welds II*. Springer Science & Business Media.

Ivanov, S.Y., Karkhin, V.A., Mikhailov, V.G., Martikainen, J. and Hiltunen, E., 2018. Assessment of the sensitivity of welded joints of al–Mg–si alloys to liquation cracks under laser welding. Metal Science and Heat Treatment, 59(11-12), pp.773-778.

Malin, V. "Study of metallurgical phenomena in the HAZ of 6061-T6 aluminum welded joints." Welding Journal-Including Welding Research Supplement 74, no. 9 (1995): 305s.

Stefanescu, D & Ruxanda, R, 2004. Solidification Structure of Aluminum Alloys, ASM Vol. 9,

Walter, V., K. A. Weidenmann, and V. Schulze. "A comparison of FSW, BHLW and TIG joints for Al-Si-Mg alloy (EN AW-6082 T6)." *Procedia CIRP* 18 (2014): 120-125.

Nguyen, T.N. and Wahab, M.A., 1998. The effect of weld geometry and residual stresses on the fatigue of welded joints under combined loading. *Journal of Materials Processing Technology*, *77*(1-3), pp.201-208.

Hobbacher, A. ed., 1996. *Fatigue design of welded joints and components: Recommendations of IIW Joint Working Group XIII-XV*. Woodhead Publishing.